HHS Public Access

Author manuscript

Mitochondrion. Author manuscript; available in PMC 2024 May 01.

Published in final edited form as:

Mitochondrion. 2023 May ; 70: 31–40. doi:10.1016/j.mito.2023.03.003.

HIV-1 gp120 protein promotes HAND through the calcineurin pathway activation

Jenny Shrestha[1,2,‡], **Maryline Santerre**[1,2], **Charles N Allen**[1,2], **Sterling P Arjona**[1,2], **Robert Hooper**[2], **Ruma Mukerjee**[1,2], **Marcus Kaul**[3,4,5], **Natalia Shcherbik**[6], **Jonathan Soboloff**[2,7], **Bassel E Sawaya**[1,2,7,¶]

[1]Molecular Studies of Neurodegenerative Diseases Lab, Lewis Katz School of Medicine - Temple University Philadelphia, PA 19140, USA

[2]FELS Cancer Institute for Personalized Medicine, Lewis Katz School of Medicine - Temple University Philadelphia, PA 19140, USA

[3]Infectious and Inflammatory Disease Center, Sanford Burnham Prebys Medical Discovery Institute, La Jolla, CA, USA

[4]Department of Psychiatry, UCSD, San Diego, CA, USA

[5]Division of Biomedical Sciences, School of Medicine, UCR, Riverside, CA, USA

[6]Department for Cell Biology and Neuroscience, School of Osteopathic Medicine, Rowan University, 2 Medical Center Drive, Stratford, NJ, 08084, USA

[7]Department of Cancer and Cellular Biology; Lewis Katz School of Medicine - Temple University Philadelphia, PA 19140, USA.

Abstract

For over two decades, highly active antiretroviral therapy (HAART) was able to help prolong the life expectancy of people living with HIV-1 (PLWH) and eliminate the virus to an undetectable level. However, an increased prevalence of HIV- associated neurocognitive disorders (HAND) was observed. These symptoms range from neuronal dysfunction to cell death. Among the markers of neuronal deregulation, we cite the alteration of synaptic plasticity and neuronal communications.

[¶]**Corresponding Author:** Bassel E Sawaya, PhD, MS(IME), MBA, Fels Institute for Cancer Research, Lewis Katz School of Medicine, Temple University. 3307 North Broad Street; Philadelphia, Pennsylvania 19140. Phone: 215-707-5446; Fax: 215-707-5948; sawaya@temple.edu.

[‡]Current address:

JS- Bristol Myers Squibb, 556 Morris Ave (Building S7), Summit, NJ 07901 (jenny.shrestha@bms.com)

[9.]AUTHORS CONTRIBUTIONS

JS, MS, CA, SA, RM, RH, NS, and MK performed the studies. JS directed the calcium studies. BES designed and directed the work and wrote the manuscript. All authors approved the submitted version.

[10.]CONFLICT OF INTEREST

The authors declare that the research was performed in absence of any financial relationships and has no potential conflict of interest.

[8.]ETHICS STATEMENT

All experiments involving gp120-tg mice were performed per NIH guidelines and approved by the IACUC of Sanford Burnham Presbys Medical Discovery Institute. Dr. Sawaya's animal protocol was approved by the Temple University IACUC.

Clinically, these dysfunctions led to neurocognitive disorders such as learning alteration and loss of spatial memory, which promote premature brain aging even in HAART-treated patients. In support of these observations, we showed that the gp120 protein deregulates miR-499-5p and its downstream target, the calcineurin (CaN) protein. The gp120 protein also promotes the accumulation of calcium (Ca^{2+}) and reactive oxygen species (ROS) inside the neurons leading to the activation of CaN and the inhibition of miR-499-5p. gp120 protein also caused mitochondrial fragmentation and changes in shape and size. The use of mimic miR-499 restored mitochondrial functions, appearance, and size. These results demonstrated the additional effect of the gp120 protein on neurons through the miR-499-5p/calcineurin pathway.

Keywords

HIV-1 gp120; Calcineurin; Fusion/Fission; neurodegenerative disease

1. Introduction

It is well-described that mitochondria integrity is critical for its functions. Along with generating ATP, mitochondrial dynamics to undergo fission and fusion to maintain their shape and activity are equally important and could be used to decipher cellular integrity (Amorim et al., 2022). Under normal physiological conditions, a delicate balance exists between fission and fusion machinery; however, during cellular stress, this dynamic is altered (Kumar and Ashraf, 2022; Scheffer et al., 2022; Spurlock et al., 2020; Uchikado et al., 2022). Altered mitochondrial dynamics have been reported in several diseases like cancer (Fontana and Limonta, 2021), pulmonary hypertension (Sharma et al., 2021), patent ductus arteriosus (Bentley et al., 2021), cardiac myopathies (Quiles and Gustafsson, 2022), and in several neurodegenerative diseases (e.g., Parkinson, Alzheimer, and Huntington) (Nabi et al., 2022).

Mitochondrial fission generates fragmented mitochondria, while mitochondrial fusion causes an elongated mitochondrial network. This phenomenon is managed by Drp1, Fis1 proteins (fission), and Mfn1, Mfn2, and Opa1 proteins (fusion) (Agarwal et al., 2016; Youle and van der Bliek, 2012). Fusion is involved in rescuing/inhibiting potential stress-induced damage and preventing the loss of mtDNA (Chen and Chan, 2010; Nhu et al., 2022). It is also required for proper mitochondrial distribution and dendritic spine outgrowth. The deletion of the Mfn2 protein leads to cerebellar neurodegeneration (Chen et al., 2007).

Mitochondrial fission, on the other hand, is critical for cell growth and development. Inhibiting Drp1 activity has neuroprotective effects both *in-vitro* and *in-vivo* in hippocampal neurons (Ali et al., 2022; Grohm et al., 2012).

There has been a tremendous effort to understand the role of mitochondrial dynamics (Liu and Yang, 2022; Xue et al., 2022); however, in the case of HIV, the mechanisms involved in mitochondrial dynamics remain unclear (Day and O'Neill, 2021; Halcrow et al., 2022). Previously, we demonstrated the effect of gp120 on mitochondrial bioenergetics and metabolic reprogramming (Allen et al., 2022a; Allen et al., 2022b; Shrestha et al., 2022); here, we focused on the effect of gp120 on upstream factors such as glutamate

excitotoxicity, ROS, and miRNAs specifically miR-499-5p; that might lead to altered mitochondrial shape by altering fission and fusion proteins that could contribute to the development of HAND.

2. MATERIALS AND METHODS

2.1. Cell culture.

The human neuroblastoma cell line (SH-SY5Y) was purchased from ATCC (CRL-2266) and grown in Dulbecco modified eagle medium: nutrient type-12 (DMEM F12) supplemented with 10% fetal bovine serum (FBS), 1% non-essential amino acid, and 1% sodium pyruvate. The cells were incubated at 37°C supplemented with 5% CO2 and passaged at 85–90% confluency. Only the cells within 10 passages from the time purchased were used. The cells were seeded at the density of 5×10^5 cells/per well for 6 well plates and differentiated with 10 μM retinoic acid (RA) treatment for at least 3–4 days.

2.2. Chemicals and gp120 treatment.

Recombinant HIV-1 gp120-IIIB was kindly received from NIH AIDS Reagent Program (Catalog # 11784). Samples were treated with 100ng/ml of gp120 for 24 or 48 hours. HIV-1 gp120-IIIB is a T-tropic protein. CXCR4 inhibitor (AMD3100, kindly received from the AIDS Reagent Program Cat # 8128) was used at a concentration of 2 mM (Donzella et al., 1998).

2.3. Transient transfection assay.

pDsRed2-Mito was purchased from Clontech (Catalog #632421). The hsa-miR-499-5p mimic (HMI0615) and mimic control were purchased from Sigma. The SH-SY5Y cells were seeded at 5×10^5/ml in the culture dishes. On the day of transfection, the cells were incubated in the OPTI MEM medium for 1 hour before transfection. For transfection, mimic-499-5p or the mimic control with the working concentration of 5 nM and dsMito-Red with 1.5 μg/μl using lipofectamine 2000; were prepared in the transfection medium (Opti MEM). The cells were then incubated for 4–6 hours at 37°C. The transfection medium Opti MEM was replaced by the differentiation medium DMEM F12 with 10 μM retinoic acid after 4–6 hours. The cells were left to differentiate for 4 days followed by the different treatment conditions specified per experiment and then subjected to the respective experiments.

2.4. Western blot assay.

The whole-cell lysate was prepared using Radioimmunoprecipitation assay (RIPA) lysis buffer (25mM Tris–HCl pH 7.6, 150mM NaCl, 1% Triton, and 0.1% SDS) + protease inhibitor and phosphatase inhibitor cocktail. Protein concentrations were estimated using a Bradford Assay (Bio-Rad Catalog # 500–0006). Lysates (25 μg) were mixed with 6X loading dye containing b-ME followed by boiling at 95°C on a dry bath, then loaded. The gel was transferred to a nitrocellulose membrane. The membrane was blocked with 5% BSA for 1 hour at room temperature. Primary antibodies were prepared in a 5% BSA solution as well and the membranes were incubated overnight at 4°C with gentle shaking. Antibodies used to detect the target proteins: MCU (Santa Cruz), MCUR1 (Santa Cruz), Calcineurin (Cell Signaling), Drp1 (Novus), phosphor-Drp1S637 (Cell Signaling), Fis1

(Santa Cruz), and NMDAR (Cell Signaling). Species-specific secondary antibodies were used from Santa Cruz and the membranes were incubated for 1 hour at room temperature. Chemiluminescence was used to detect the signal. The densitometry ratio of the bands was determined using an ImageJ that was normalized to GAPDH.

2.5. RNA extraction.

Total RNA was extracted from the sample treated with different conditions using the SurePrep TrueTotal RNA purification kit from Fisher Bioreagents as per the manufacturer's instructions. Nanodrop was used to determine the purity and concentration of the RNA extracted.

2.6. miRNA.

For microRNA expression cDNA was synthesized using miRCURY LNA Universal RT microRNA PCR from EXIQON with 100 ng of RNA. Primers for miR-499-5p were purchased from Exiqon. U6 was used as an internal control.

2.7. mRNA Gene Expression.

cDNA was synthesized using a SuperScript VILO cDNA synthesis kit (Invitrogen 11754–050). Following primers were purchased from IDT: DRP1: (F- 5'-acttgacctccctactggc-3'); (R- 5'-tcctctatcccgttgacacc-3'); GAPDH: (F- 5′-gccttccgtgttcctacc-3'); (R- 5′-cctcagtgtagcccaagatg-3')

2.8. ROS assay.

The trafficking of 2,3,4,5,6-pentafluorodihydro-tetramethylfosamine (redox sensor red CC-1; Invitrogen) was used to detect reactive oxygen intermediates. Redox Sensor Red CC-1 is oxidized in the cytosol and accumulates in either the mitochondria or the lysosomes depending on the oxidation of the cell. Thus, Redox Sensor Red is a measurement of redox potential. Differentiated SH-SY5Y cells under different treatment conditions were incubated for 5 minutes with 1μM of Redox Sensor Red CC-1 and a mitochondria-specific dye, MitoTracker Green FM (25 nM, Molecular Probes). 100 nM H_2O_2 was used as a positive control. Culture slides were washed with 1X PBS and visualized using an EVOS cell imaging system. If Redox Sensor Red is co-localized with MitoTracker Green in the mitochondria, then the oxidation level of the cell is high. Note that all ROS measurement experiments were performed at least three times.

2.9. Immunofluorescence assay.

Cells were fixed with 2% paraformaldehyde for 3 minutes, followed by rinsing with 1X PBS, and blocked with 1% BSA for 1 hour. Next, they were incubated in a specific primary antibody (Fis1 and Drp1) (1:100 dilutions) overnight at 4°C followed by incubation in a fluorescein-tagged secondary antibody for 1 hour at room temperature. The cells were then washed and mounted in DAPI containing medium. Leica EL600 DMI3000 confocal microscopy system was used to visualize them.

2.10. Immunohistochemistry:

Gp120 transgenic mice brain.—Imaging for gp120-tg mice brains (HPX1481) and WT (HPX1477) was done in Dr. Kaul's Lab (Sanford Burnham Presbys Medical Discovery Institute). WT and gp120 tg mice were provided by Dr. Lennart Mucke (Gladstone Institute of Neurological Disease, University of California) (Toggas et al., 1994). The mice were 9 months of age for both WT and gp120-tg where they were anesthetized with Isoflurane and transcardially perfused with 0.9% saline. The brains were quickly removed and fixed with 4% paraformaldehyde for 48 hours at 4°C. The brain sections (frontal cerebral cortex layer III) of 5 μm thickness were obtained for the histological studies. The slides were permeabilized with 1% Triton X-100 for 30 mins followed by blocking with 10% heat-inactivated goat serum in PBS containing 0.5% Tween-20 for 1.5 hours. The sections were then stained with Calcineurin (Cell Signaling) and MAP-2 (Sigma) overnight followed by Alexa Flour 488-labeled goat anti-rabbit (Molecular Probes). Nuclear DNA was labeled with H33342. Per animal, at least three sagittal sections were analyzed, and, in each section, five fields were recorded using Zeiss inverted Axiovert 100M fluorescence microscope. Fluorescence and volumetric quantitation were performed with the Slide book software package.

2.11. Glutamate Assay.

Glutamate level was measured using the Glutamate Assay Kit from BioVision-MA (Catalog #K629-100) following the manufacturer's instruction. Cells treated under different conditions were homogenized in 100 μl Assay buffer and centrifuged at 13,000g for 10 minutes to remove any insoluble materials. 10 μl of each sample was used in a 96-well plate, then, 40 μl of the assay buffer was added to each plate to bring the volume to 50 μl. The reaction mix was prepared as indicated and 100 μl of it was added to each well on the standard set and the sample set. The mix was incubated at 37°C for 30 minutes protected from the light. The signal was measured at OD=450 nM using a Modulus microplate reader. The data is presented in a relative form as compared to the untreated control.

2.12. Calcium measurement.

The SH-SY5Y cells were grown on poly-D-Lysine coated coverslips and differentiated for at least 72 hours. The cells were untreated (control) or treated with gp120 for 3 hours before transferring to a cation-safe buffer (10mM NaCl, 7.2mM KCl, 1.2mM $MgCl_2$, 11.5mM Glucose, 20mM HEPES-NaOH, 1mM $CaCl_2$, pH 7.2) and loaded with Fura2-acetoxymethylester (Fura2-AM; 2 μM) for 30 min at 24°C as previously described (Go et al., 2019; Hooper et al., 2015) followed by 10 mM rhod-2 AM (Invitrogen) and incubated at 37°C, 5% CO_2 for 1 hour. Cells were washed and allowed to de-esterify for a minimum of 30 min at 24°C. Ca^{2+} measurements were made using a Leica DMI 6000B fluorescence microscope controlled by Slidebook Software (Intelligent Imaging Innovations; Denver, CO). Fura2 fluorescence emissions were measured at 505 nm while alternating between 340 and 380 nm excitation wavelengths at a frequency of 0.67 Hz; cytosolic Ca^{2+} measurements are shown as 340/380nm ratios obtained from groups (35 to 45) of single cells. Rhod-2 fluorescence emissions at 605 nm were monitored after 546 nm excitation at a frequency of 0.67 Hz. To induce store-operated Ca^{2+} entry, the function of SERCA was inhibited by the

addition of thapsigargin (Tg: 2 μM) followed by the addition of 1 mM Ca^{2+} after recovery of cytosolic Ca^{2+} content.

2.13. Mitochondria membrane potential.

Mitochondrial membrane potential was measured using the guava MitoPotential assay which is based on fluorescence. JC-1, a cationic dye, changes color with the change in the membrane potential to either green or orange. The polarized mitochondria caused JC-1 to accumulate in the mitochondria forming J-aggregates and fluoresce orange (~590nm) and with the loss of the membrane potential, the mitochondria become depolarized thus losing the concentration of the dye and dissociation of the J-aggregates and will fluoresce green (~530 nm). The differentiated SH-SY5Y cells with different treatment conditions were seeded at 1×10^6 cells/ml. After the treatment, the cells were trypsinized and re-suspended in the warm DMEM F-12 medium containing 2 μM of JC-1 and incubated in a 96-well microplate for 30mins. Carbonyl cyanide *m*-chlorophenyl hydrazine (CCCP) was used as a control for membrane depolarization. Guava easyCyte HT system was used to measure the mitochondrial membrane polarization (MMP) and the data were analyzed with the software provided by Guava easyCyte 2.7.

2.14. Statistical Analysis.

All the experiments were repeated at least in triplicate. Statistical analysis was performed using a one-way analysis of variance with a *post hoc* Student's *t*-test. Data are expressed as the mean of ± S.D. Results were judged statistically significant if $p<0.05$ by analysis of variance. (Marked in the figure as *p<0.05; **p<0.01; ***p<0.001 where needed). Data were plotted either using GraphPad Prism version 5.0 or 7.0.

3. RESULTS

gp120 protein deregulates Ca^{2+} homeostasis in human neurons.

To determine how gp120 affects Ca^{2+} homeostasis in human neurons, we monitored its effects on both cytosolic and mitochondrial Ca^{2+} levels by fluorescence microscopy using Fura2 and Rhod2, respectively. SH-SY5Y cells were differentiated and treated with recombinant gp120 protein for 3 hours. No changes in basal cytosolic Ca^{2+} content were observed, however, gp120 caused a marked decrease in basal mitochondrial Ca^{2+} content (Fig 1A). Thapsigargin (Tg) is a Sarcoplasmic/ER Ca^{2+} ATPase inhibitor used to deplete the ER Ca^{2+} store which stimulates store-operated Ca^{2+} entry (SOCE), detected by the addition of 1mM Ca^{2+}. While there were no gp120-induced differences in ER Ca^{2+} content (based on Tg-induced Ca^{2+} release), increased SOCE was observed in gp120-treated cells (Fig 1A; grey lines). While mitochondrial Ca^{2+} levels followed a similar pattern in the presence or absence of gp120, mitochondrial Ca^{2+} content was consistently lower after the gp120 treatment (Fig 1A; red lines). Decreased mitochondrial Ca^{2+} content can lead to the upregulation of NMDA receptors to facilitate additional Ca^{2+} entry into the cells as a compensatory mechanism. Hence, we determined the expression levels of NMDA receptors.

gp120 treatment increases the expression of NMDAR and glutamate levels.

To determine if the addition of gp120 protein induces neuronal deregulation through the activation of NMDAR and causes an increase in intracellular calcium (Haughey and Mattson, 2002; Hoke et al., 2009; Sanchez et al., 2016; Xu et al., 2011), we examined the expression levels of NMDAR. SH-SY5Y cells were differentiated and treated with 100 ng/ml of recombinant gp120 protein for 24 hours. The cell extracts were collected and subjected to Western blot analysis using anti-NMDAR antibodies. As shown in Fig 1B, the expression level of NMDAR protein increased in gp120-treated cells compared to the control untreated.

Increased NMDAR expression and activity are often associated with glutamate release and potential toxicity (Bachis and Mocchetti, 2004; Jadhav and Nema, 2021; Potter et al., 2013). As a neurotransmitter, glutamate is released from a pre-synaptic neuron to stimulate the post-synaptic neuron; hence, we measured its levels. The cells were differentiated and treated with 100 ng/ml of recombinant gp120 protein for 24 hours. The glutamate level was measured using a colorimetric glutamate assay kit. As shown in Fig 1C, a significant increase in glutamate level was observed in gp120-treated cells compared to the control untreated.

Along with NMDAR activation, a flux of extracellular calcium into the cell activates calpain expression (del Cerro et al., 1994; Ferragamo et al., 2009; Lai et al., 2014). To corroborate these. results, we evaluate the expression of calpain protein in gp120-treated SH-SY5Y. The cells were differentiated and treated with 100 ng/ml of recombinant gp120 protein for 24 hours. The cells were collected, and protein extracts were subjected to Western blot analysis. As shown in Fig 1D, the addition of gp120 protein led to increased calpain expression, indicating that the Ca^{2+}-dependent mechanism might be involved.

Overall, data from Figure 1 showed that the addition of gp120 protein deregulates mitochondrial calcium homeostasis, activates the NMDA receptor, and increases expressions of calpain and glutamate.

gp120 disturbs the mitochondrial uniporter complex expression levels.

Decreased mitochondrial calcium (Fig 1A) gave the rationale to measure expression levels of the mitochondrial uniporter MCU and MCUR. The mitochondrial uniporter complex is present in the inner mitochondrial membrane and is involved in Ca^{2+} transport into the mitochondria. Increased Ca^{2+} influx has been linked to mitochondrial damage and cellular deregulation in neurons (Kawamata and Manfredi, 2010). To validate this observation, we examined the status of proteins involved in mitochondrial calcium entry. Differentiated SH-SY5Y cells were treated with 100 ng/mL of gp120 protein for 24 hours. The cells were collected and subjected to Western blot analysis using anti-MCU and MCUR1 antibodies. As shown in Fig 2A, increased expression of both MCU and MCUR1 was observed in gp120-treated cells compared to the control untreated, confirming their role in gp120-mediated Ca^{2+} entry in the mitochondria. Panel B represents the quantification of MCU and MCUR1 expressions.

HIV-gp120 promotes ROS accumulation.

Calcium flux regulates mitochondrial reactive oxygen species (ROS); hence, we measured ROS levels in gp120-treated SH-SY5Y cells using the RedoxSensor Red dye. RedoxSensor Red dye localizes to the cytosol, mitochondria, or lysosomes. In the presence of gp120, the total ROS levels, indicated by the RedoxSensor Red fluorescence intensity, were significantly elevated compared to control cells (Fig 1C). We also labeled mitochondria with a counterstain (MitoTracker Green), so the colocalization of the RedoxSensor Red and MitoTracker Green can be imaged and visualize redox potential in the mitochondria. The addition of gp120 increased the colocalization of RedoxSensor (red) and MitoTracker (green), suggesting that mitochondrial ROS also increased in these cells (Figs 1C, D). The Redox Red dye accumulated in the mitochondria of cells treated with HIV-1 gp120 and H_2O_2 (used as a positive control) indicates a high redox potential of the cytosol in these cells (supported by the colocalization of the redox red and mito green dyes). Disturbance in mitochondrial ROS can act on mitochondrial fusion and fission proteins resulting in fragmented mitochondria.

gp120 treatment leads to altered mitochondrial morphology.

Mitochondria are highly dynamic and often undergo fission and fusion to meet the energy demand of the cells. However, during stress conditions, their dynamics are altered. Further, smaller, swollen, and fragmented mitochondria were observed in the stressed cell compared to elongated worm-like structure mitochondrial shape in the control cells (Bottone et al., 2013; Khasho et al., 2015; Wiemerslage and Lee, 2016). Oxidative stress has been reported as one of the major factors altering mitochondrial morphology (Ahmad et al., 2013; De Gaetano et al., 2021). Therefore, we examined the impact of gp120 protein on the mitochondrial shape. SH-SY5Y cells were transfected with dsMito-RED to visualize the mitochondria followed by differentiation and then treated with gp120 (100 ng/ml for 24 hours). Using a confocal microscope (Leica EL600 DMI3000), we visualized small, round, and short with a bleb shape mitochondrion in gp120-treated cells compared to tubular and long mitochondria in the control (Fig 3A). Small and round mitochondria have been reported in the visual cortex and the hippocampus of Alzheimer's postmortem brain patients as compared to the control along with fragmented Golgi bodies and reduced synaptic profile (Baloyannis SJ, 2011). Also, mitochondrial volume and distribution seem to be altered in gp120-treated cells compared to the control (Fig 3A). Decreased mitochondrial volume and altered mitochondrial shape (donut vs straight or curved) have been associated with decreased synaptic vesicles (Ivannikov et al., 2013) and impaired memory (Hara et al., 2014). These observations indicate that gp120 deregulates mitochondrial shape and volume in the neurons and corroborate previous studies (Khacho et al., 2015).

gp120 deregulated mitochondrial fission and fusion protein expression.

The mitochondrial shape is regulated by several fission and fusion proteins. Since we observed small and round mitochondria, we examined the expression of the proteins involved in fission and fusion. Differentiated SH-SY5Y cells were treated with recombinant gp120 protein for 24 hours, then subjected to Western blot analysis using anti- Drp1, -pDrp1^{S637}, and -Fis1 antibodies. We observed an increased expression of Drp1 and Fis1

proteins in gp120-treated cells compared to the Control, but a decreased phosphorylation of pDrp1^{S637} (Fig 3B). Panel C represents the quantification of Drp1, pDrp1, and Fis1 expression levels. Note that Drp1^{S637} phosphorylation increases the dissociation of Drp1 from mitochondria and inhibits mitochondrial fission (Kashatus et al., 2011; Wang et al., 2012), while its dephosphorylation facilitates its translocation to mitochondria and subsequently increases mitochondrial fission, (Campello and Scorrano, 2010).

We confirmed the Western results using an immunocytochemistry assay. We transfected the cells with pDsRED Mito, differentiate them, then treated them with recombinant gp120 protein. The cells were probed with either Drp1 or Fis1 antibodies followed by Alexa 488 (secondary antibody). Figures 3D and E showed the increased expression (green) and mitochondrial localization (yellow-orange) of Drp1 and Fis1, respectively, in gp120-treated cells versus the untreated control. These data suggest that the addition of gp120 protein alters mitochondrial morphology by targeting fission proteins such as Drp1 and Fis1.

gp120 deregulates the expression levels of Calcineurin and miR-499-5p.

To better understand the mechanism used by gp120 in deregulating the fission proteins, we examined the upstream regulator of Drp1. The activity of Drp1 depends on its phosphorylation on serine residues 637 and 616, which are regulated by several kinases and phosphatases (Knott et al., 2008). Phosphorylation of Drp1 on serine residue 637 causes its translocation from the cytosol to the mitochondria outer membrane (OMM), which could be neutralized by the Ca^{2+}-dependent phosphatase, calcineurin (CaN) (Cereghetti et al., 2008). SH-SY5Y cells were differentiated and treated with recombinant gp120 protein, then subjected to Western blot analysis using an anti-CaN antibody. As shown in Fig 4A, the expression level of CaN alpha protein increases in gp120-treated cells compared to the untreated group. These results were confirmed using brain tissues prepared from gp120-transgenic mice. As shown in Fig 4B, the expression level of CaN alpha protein increases in gp120-tg mice compared to the control mice. Panel C represents the quantification of CaN-α expression in mice brains.

The calcium-dependent phosphatase, Calcineurin, is activated following increased cytosolic Ca^{2+}, which is triggered by the collapse of the mitochondrial membrane potential (Cereghetti et al., 2008). To corroborate these results, we measured the mitochondrial membrane potential using differentiated SH-SY5Y cells treated with gp120 protein and the control. Indeed, the addition of gp120 protein decreased the mitochondrial membrane potential compared to the untreated cells (Fig 4D). These results support the increased calcineurin expression.

Further, calcineurin is a direct target of miR-499-5p. This miRNA (miR-499-5p) has been shown to have a protective effect in cardiomyocytes and regulates mitochondrial fission and fusion by targeting the calcineurin gene and inhibiting its activity along with its downstream target Drp1 (Wang et al., 2011). The role of miR-499-5p in the brain was established in neuropsychiatric disorders and hypoxic-ischemic encephalopathy (Banigan et al., 2013; Jia et al., 2020; Smalheiser et al., 2014). This gave us the rationale to examine the expression level of miR-499-5p in differentiated SH-SY5Y cells treated with gp120

protein. We observed a decrease in miR-499-5p expression (Fig 4E). Hence, we concluded that gp120 alters mitochondrial shape via inhibition of miR-499-5p.

Overexpressing miR-499-5p downregulates the Calcineurin and Drp1 expression levels.

To further determine whether gp120 is deregulating Calcineurin and Drp1 via miR-499-5p, we transfected SH-SY5Y cells in duplicate with 5nM of the mimic-499-5p or the control RNA (scrambled or sRNA) followed by differentiation and gp120 treatment as described in the Methods section. RNA was collected from the first set and subjected to RT-qPCR, while protein extracts were collected from the second set and used for Western blot analysis using an anti-calcineurin antibody. As shown in Fig 5A, gp120 protein decreased the expression level of endogenous miR-499-5p but failed to do so in cells transfected with the mimic499-5p. The addition of gp120 protein did not affect the endogenous level of miR-499-5p in cells transfected with the scrambled RNA. Similarly, overexpression of mimic miR-499-5p led to decreased expression levels of Calcineurin (Fig 5B) and Drp1 (Fig 5C) proteins.

Next, we transfected the cells with the mimic and examined the shape of the mitochondria. As indicated in Fig 5D, the cells transfected with the mimic have long mitochondria. The mimic499-5p also prevented the rounding of mitochondria in gp120-treated cells. These data point to a potential role of miR-499-5p in deregulating mitochondrial dynamics and shape via a Calcineurin-dependent mechanism.

4. DISCUSSION

Here, we focused on the mechanism used by the HIV-gp120 protein to alter mitochondrial functions, a phenomenon that could promote HIV-1-associated neurocognitive disorders (HAND). We previously demonstrated that the gp120 protein affects neuronal functions through CREB dephosphorylation (Shrestha et al., 2022). While here, we added the involvement of miR-499-5p (Fig 6). Indeed, while the gp120 protein changes mitochondrial shape, fusion, fission, and movement, it failed to do so in the presence of miR-499-5p.

Interestingly, treatment of neuronal cells with gp120 protein increases calcium flux, which leads to miR499-5p functional inhibition. We demonstrated that gp120 protein increases the NMDAR protein expression (Fig1 A) and glutamate levels (Fig 1B), suggesting a role for gp120 in the hyperactivation of NMDAR. Forward trafficking and clustering of NMDAR on the cell surface have been reported in gp120-treated cells (Xu et al., 2011). Our data corroborate the literature where NMDAR antagonists protect against gp120-induced cognitive disorders in rat neurons (Zeng et al., 2022; Zhou et al., 2017). Our results are not unprecedented. Studies showed that the HIV-1 Tat protein activates the NMDAR receptor and increases Ca^{2+} flux in neurons (Krogh et al., 2015).

The glutamate level depends on the glutamate transporter ability (EAAT2) to clear secreted extracellular glutamate and minimizes glutamate toxicity. Interestingly, the EAAT2 receptor activity decreases in the brains of patients suffering from neurodegenerative diseases or AIDS. Hence, causing an excess in intracellular glutamate and increased hyperactivity of NMDAR (Fernandes et al., 2007; Wang et al., 2003; Ye et al., 2017).

One of the outcomes of NMDAR hyperactivity is the influx of Ca^{2+}, which is associated with Ca^{2+}/calmodulin-dependent kinase II (CaMKII)-mediated increase in phosphorylation of AMPA (glutamate) receptors (Barria et al., 1997). AMPA receptors (AMPARs) are tetrameric ion channels assembled from GluA1-GluA4 subunits that mediate most synaptic transmission in the brain. In the hippocampus, most synaptic AMPARs are composed of GluA1/2 or GluA2/3. Phosphorylation of GluA1 S831 and S845 by the cAMP-dependent protein kinase (PKA) and CAMKII prime extra-synaptic receptors for synaptic insertion in response to NMDA receptor Ca^{2+} signaling during long-term potentiation (LTP). On the other hand, CaNα dephosphorylates GluA1 on S831 and S845, causing long-term depression (LTD) (Sanderson et al., 2012). Indeed, we showed that adding gp120 protein alters synaptic plasticity (Shrestha et al.,2022).

Further, we found that gp120 causes intracellular Ca^{2+} increase (Fig 2A), which leads to increased mitochondrial ROS production (Fig 2D) and activation of the calpain pathway. These results are not unprecedented; several labs, including ours, showed that the addition of viral proteins to neurons increases calcium secretion (Chang et al., 2011; Hu X, 2016; Kim et al., 2018; Nath et al., 1995; Rom et al., 2009; Weissman et al., 1997). Also, neuronal treatment with gp120 protein increased the expression levels of MCU and MCUR1 proteins (Fig 2B). MCU is the pore-forming subunit through which the Ca^{2+} enter (Chaudhuri et al., 2013), while MCUR1, the integral membrane protein that binds to MCU, is required for MCU-dependent Ca^{2+} entry into the mitochondria (Shanmughapriya et al., 2015). MCUR1 knockdown alters MCU-dependent Ca^{2+} uptake (Mallilankaraman et al., 2012). These results suggest that both proteins are involved in HIV-1-induced mitochondrial Ca^{2+} entry. Here, we only examined the expression levels of MCU and MCUR1 proteins because they are essential for MCU complex assembly (Tomar et al., 2016). However, other proteins in the complex that plays a role as Ca^{2+} sensors and regulate the entry, like EMRE and MICU, should be studied to understand the function of the MCU complex in HAND.

Moreover, gp120 promotes changes in mitochondria shape (blebbed, rounded, and donut-shaped structure). These changes are often observed in neurodegenerative diseases (Gao et al., 2001; Lu et al., 2007). Further, increased ROS (Fig 2C) could change mitochondria shape, decrease mitochondrial membrane potential (Fig 4D), and alter fission and fusion proteins (Drp1, Fis1, Opa-1, or Mfn-2) activities. Furthermore, decreased ATP and MMP, and ROS generation has often been referred to as the vicious cycle (Sanz et al., 2006), where one can affect the others, leading to a complex mechanism of mitochondrial deregulation. These results also point to a disrupted function of the RhoT1/Miro1 protein, which is deregulated following the loss of mitochondrial membrane potential and indicates a problem with mitochondrial movement (Grossmann et al., 2020; Shrestha et al., 2022).

As we previously showed, the gp120 protein causes a loss of mitochondrial dynamics (Shrestha et al., 2022), which can cause aberrant fission and fusion leading to neuronal damage (Knott et al., 2008). Indeed, we observed an increase in Drp1 expression levels along with another fission protein, Fis1, in gp120-treated cells (Fig 3B), indicating possible increased fission leading to the above-observed phenotype (mitochondrial shape). Once activated, the cytosolic protein Drp1 translocates to the mitochondrial outer membrane (OMM). The binding of Drp1 to the OMM is mediated by the mitochondrial fission factor

(Mff) (Otera et al., 2010). Drp1 translocation also depends on the mitochondrial outer membrane proteins such as Miff, MiD49, and Fis1.

The role of Fis1 in recruiting Drp1 to the OMM remains unclear; however, adding gp120 protein increases the expression level of both proteins (Figs 3B–E). In the case of HIV-1, one study contradicts our findings, where the authors reported decreased Drp1 expression in the HIV-1 brain and possible increased fusion (Fields et al., 2016), while other studies corroborate our data (Kanda et al., 2016; Teodorof-Diedrich and Spector, 2018).

Although this study lacks human samples, our results corroborate data regarding other neurodegenerative diseases where increased mitochondrial fission was reported. Alzheimer's mice model showed increased expression of fission genes and proteins and decreased fusion genes and proteins, causing shorter and fragmented mitochondria. The same study also reported that this phenomenon precedes decreased synaptic formation observed via decreased PSD-95 (Calkins et al., 2011). These studies support our published data showing decreased pre- and post-synaptic proteins with gp120 treatment (Shrestha et al., 2022). Increased fission also suggests a possible autophagy/mitophagy involvement leading to aberrant-shaped mitochondria in gp120-treated cells.

Further, Drp1 activation depends on its phosphorylation status. Loss of Drp1 phosphorylation on serine residue 637 by calcineurin causes its translocation to the outer mitochondrial membrane and increases mitochondrial fission (Cereghetti et al., 2008), leading to increased neurodegenerative diseases, and cancer. It also triggers mitochondrial fragmentation, uncontrolled cell cycle, and alters the metabolic cycle (Serasinghe and Chipuk, 2017), which we previously described and published (Allen et al., 2022, Shrestha et al., 2022). These results also confirm that gp120 is involved in spatial memory impairment since excessive mitochondrial fission plays a role in synaptic depression and cognitive impairment in an AD model (Baek et al., 2017). Based on the literature, increased cytosolic Ca^{2+} activates calcineurin and triggers the collapse of the mitochondrial membrane potential activation (Cereghetti et al., 2008). Adding gp120 protein corroborates the results in Figures 4A–C using neuronal cells line and gp120-tg mice. This observation was reversed in the presence of mimic miR-499, confirming the importance of this miRNA in HAND pathology. Indeed, restoring miR-499-5p expression and function plays a therapeutic role in heart disease (Wang and Wu, 2022), and protects against lung injury (Zhang et al., 2021), and hypoxic-ischemic encephalopathy (Jia et al., 2020).

The Calcineurin-Drp1 pathway also plays a role in Parkin-mediated mitochondrial fission in a Parkinson's model, in heart disease, AD, and now in HIV-1 (Baek et al., 2017; Buhlman et al., 2014; Tangmansakulchai et al., 2016; Wang et al., 2011). Inhibition of CaN reverses this pathway in all the above diseases, as confirmed in our data. Increased calcineurin expression can also dephosphorylate the CREB protein leading to CREB loss of function and memory impairment, which corroborates our data (Kim and Seo, 2011, Shrestha et al., 2022).

Overall, our results provide insight into the players involved in mitochondrial deregulation in gp120-treated cells. Altered fission and fusion lead to changes in mitochondrial density and bioenergetics. This was linked to memory impairment and learning disability in monkeys

and mice (Hara et al., 2014; Ivannikov et al., 2013) and could be one of the factors causing similar effects in the brain of PLWH, and gp120 is one of the viral proteins responsible for these alterations. Therefore, identifying and targeting factors like miR-499-5p could present a potential therapy to prevent HAND pathology.

ACKNOWLEDGMENTS

The following reagents were obtained through the NIH AIDS Reagent Program, Division of AIDS, NIAID, NIH: HIV-1 gp120 (subtype B HIV-1_{IIIB} gp120 Protein, Recombinant from CHO Cells, ARP-11784, contributed by DAIDS, NIAID; produced by ImmunoDX, LLC).

5. FUNDING

This work was supported by an NIH-NIA grant AG054411 awarded to BES, and NIH grants MH087332, MH104131, MH105330, and P50 DA026306 (P5) to MK. This work was also supported by previous NIH grants NS076402 and MH093331 awarded to BES.

7. DATA AVAILABILITY STATEMENT

All processed data are included in this manuscript. Raw data, further information, or reagents contained within the manuscript are available upon request from the corresponding author, Bassel E Sawaya, sawaya@temple.edu.

11. REFERENCES

Agarwal S, Yadav A, Tiwari SK, Seth B, Chauhan LK, Khare P, Ray RS, Chaturvedi RK Dynamin-related Protein 1 Inhibition Mitigates Bisphenol A-mediated Alterations in Mitochondrial Dynamics and Neural Stem Cell Proliferation and Differentiation. J. Biol. Chem, 291(2016), pp. 15923–39. [PubMed: 27252377]

Ahmad T, Aggarwal K, Pattnaik B, Mukherjee S, Sethi T, Tiwari BK, Kumar M, Micheal A, Mabalirajan U, Ghosh B, Sinha Roy S, Agrawal A Computational classification of mitochondrial shapes reflects stress and redox state. Cell Death Dis, 4(2013), pp. e461. [PubMed: 23328668]

Ali M, Tabassum H, Alam MM, Parvez S N-acetyl-L-cysteine ameliorates mitochondrial dysfunction in ischemia/reperfusion injury via attenuating Drp1 mediated mitochondrial autophagy. Life Sci, 293 (2022), pp. 120338. [PubMed: 35065167]

Allen CNS, Arjona SP, Santerre M, De Lucia C, Koch WJ, Sawaya BE Metabolic Reprogramming in HIV-Associated Neurocognitive Disorders. Front. Cell. Neurosci, 16 (2022), pp. 812887. [PubMed: 35418836]

Allen CNS, Arjona SP, Santerre M, Sawaya BE Hallmarks of Metabolic Reprogramming and Their Role in Viral Pathogenesis. Viruses, 14 (2022), pp. 602. [PubMed: 35337009]

Amorim JA, Coppotelli G, Rolo AP, Palmeira CM, Ross JM, Sinclair DA. Mitochondrial and metabolic dysfunction in ageing and age-related diseases. Nat. Rev. Endocrinol, 18 (2022), pp. 243–258. [PubMed: 35145250]

Bachis A, Mocchetti I The chemokine receptor CXCR4 and not the N-methyl-D-aspartate receptor mediates gp120 neurotoxicity in cerebellar granule cells. J. Neurosci. Res, 75(2004), pp. 75–82. [PubMed: 14689450]

Baek SH, Park SJ, Jeong JI, Kim SH, Han J, Kyung JW, Baik SH, Choi Y, Choi BY, Park JS, Bahn G, Shin JH, Jo DS, Lee JY, Jang CG, Arumugam TV, Kim J, Han JW, Koh JY, Cho DH, Jo DG Inhibition of Drp1 Ameliorates Synaptic Depression, Aβ Deposition, and Cognitive Impairment in an Alzheimer's Disease Model. J. Neurosci, 37(2017), pp. 5099–5110. [PubMed: 28432138]

Baloyannis SJ Mitochondria are related to synaptic pathology in Alzheimer's disease. Int. J. Alzheimers Dis, 2011(2011), pp. 305395. [PubMed: 21922047]

Banigan MG, Kao PF, Kozubek JA, Winslow AR, Medina J, Costa J, Schmitt A, Schneider A, Cabral H, Cagsal-Getkin O, Vanderburg CR, Delalle I Differential expression of exosomal microRNAs in

prefrontal cortices of schizophrenia and bipolar disorder patients. PLoS One, 8(2013), pp. e48814. [PubMed: 23382797]

Barria A, Muller D, Derkach V, Griffith LC, Soderling T Regulatory phosphorylation of AMPA-type glutamate receptors by CaMKII during longterm potentiation. Science, 276(1997), pp. 2042–45. [PubMed: 9197267]

Bentley RET, Hindmarch CCT, Dunham-Snary KJ, Snetsinger B, Mewburn JD, Thébaud A, Lima PDA, Thébaud B, Archer SL The molecular mechanisms of oxygen-sensing in human ductus arteriosus smooth muscle cells: A comprehensive transcriptome profile reveals a central role for mitochondria. Genomics, 113 (2021), pp.3128–3140. [PubMed: 34245829]

Bottone MG, Santin G, Aredia F, Bernocchi G, Pellicciari C, Scovassi. A.I. Morphological Features of Organelles during Apoptosis: An Overview. Cells, 2(2013), pp. 294–305. [PubMed: 24709702]

Buhlman L, Damiano M, Bertolin G, Ferrando-Miguel R, Lombès A, Brice A, Corti O Functional interplay between Parkin and Drp1 in mitochondrial fission and clearance. Biochim. Biophys. Acta, 1843(2014), pp. 2012–26. [PubMed: 24878071]

Calkins MJ, Manczak M, Mao P, Shirendeb U, Reddy PH Impaired mitochondrial biogenesis, defective axonal transport of mitochondria, abnormal mitochondrial dynamics and synaptic degeneration in a mouse model of Alzheimer's disease. Hum. Mol. Genet, 20(2011), pp. 4515–29. [PubMed: 21873260]

Campello S, Scorrano L Mitochondrial shape changes: orchestrating cell pathophysiology. EMBO Rep, 11(2010), pp. 678–684. [PubMed: 20725092]

Cereghetti GM, Stangherlin A, Martins de Brito O, Chang CR, Blackstone C, Bernardi P, Scorrano L Dephosphorylation by calcineurin regulates translocation of Drp1 to mitochondria. Proc. Natl. Acad. Sci. USA, 105(2008), pp. 15803–8. [PubMed: 18838687]

Chang JR, Mukerjee R, Bagashev A, Del Valle L, Chabrashvili T, Hawkins BJ, He JJ, Sawaya BE HIV-1 Tat protein promotes neuronal dysfunction through disruption of microRNAs. J. Biol. Chem, 286(2011), pp. 41125–34. [PubMed: 21956116]

Chaudhuri D, Sancak Y, Mootha VK, Clapham DE MCU encodes the pore conducting mitochondrial calcium currents. Elife, 2(2013), pp. 00704.

Chen H, Chan DC Physiological functions of mitochondrial fusion. Ann. NY. Acad. Sci, 1201 (2010), pp. 21–5. [PubMed: 20649534]

Chen H, McCaffery JM, Chan DC Mitochondrial fusion protects against neurodegeneration in the cerebellum. Cell, 130 (2007), pp. 548–62. [PubMed: 17693261]

Day EA, O'Neill LAJ Targeting mitochondria to beat HIV-1. Nat. Immunol, 22 (2021), pp. 398–399. [PubMed: 33767428]

De Gaetano A, Gibellini L, Zanini G, Nasi M, Cossarizza A, Pinti M Mitophagy and Oxidative Stress: The Role of Aging. Antioxidants (Basel), 10(2021), pp. 794. [PubMed: 34067882]

del Cerro S, Arai A, Kessler M, Bahr BA, Vanderklish P, Rivera S, Lynch G Stimulation of NMDA receptors activates calpain in cultured hippocampal slices. Neurosci. Lett, 167(1994), pp. 149–52. [PubMed: 8177514]

Donzella GA, Schols D, Lin SW, Esté JA, Nagashima KA, Maddon PJ, Allaway GP, Sakmar TP, Henson G, De Clercq E, Moore JP AMD3100, a small molecule inhibitor of HIV-1 entry via the CXCR4 co-receptor. Nat Med, 4 (998), pp, 72–7. [PubMed: 9427609]

Fernandes SP, Edwards TM, Ng KT, Robinson SR HIV-1 protein gp120 rapidly impairs memory in chicks by interrupting the glutamate-glutamine cycle. Neurobiol. Learn. Mem, 87(2007), pp. 1–8. [PubMed: 16714124]

Ferragamo MJ, Reinardy JL, Thayer SA Ca2+-dependent, stimulus-specific modulation of the plasma membrane Ca2+ pump in hippocampal neurons. J. Neurophysiol, 101(2009), pp. 2563–71. [PubMed: 19244356]

Fields JA, Serger E, Campos S, Divakaruni AS, Kim C, Smith K, Trejo M, Adame A, Spencer B, Rockenstein E, Murphy AN, Ellis RJ, Letendre S, Grant I, Masliah E HIV alters neuronal mitochondrial fission/fusion in the brain during HIV-associated neurocognitive disorders. Neurobiol. Dis, 86(2016), pp. 154–69. [PubMed: 26611103]

Fontana F, Limonta P The multifaceted roles of mitochondria at the crossroads of cell life and death in cancer. Free Radic. Biol. Med, 176 (2021), pp. 203–221. [PubMed: 34597798]

Gao W, Pu Y, Luo KQ, Chang DC Temporal relationship between cytochrome c release and mitochondrial swelling during UV-induced apoptosis in living HeLa cells. J. Cell. Sci, 114(2001), pp. 2855–62. [PubMed: 11683418]

Go CK, Hooper R, Aronson MR, Schultz B, Cangoz T, Nemani N, Zhang Y, Madesh M, Soboloff J The Ca^{2+} export pump PMCA clears near-membrane Ca^{2+} to facilitate store-operated Ca^{2+} entry and NFAT activation. Sci. Signal, 12(2019), pp. eaaw2627. [PubMed: 31594854]

Grohm J, Kim SW, Mamrak U, Tobaben S, Cassidy-Stone A, Nunnari J, Plesnila N, Culmsee C Inhibition of Drp1 provides neuroprotection in vitro and in vivo. Cell Death Differ, 19 (2012) pp. 1446–58. [PubMed: 22388349]

Grossmann D, Berenguer-Escuder C, Chemla A, Arena G, Krüger R The Emerging Role of RHOT1/Miro1 in the Pathogenesis of Parkinson's Disease. Front. Neurol, 11(2020), pp. 11:587. [PubMed: 32047473]

Halcrow PW, Kumar N, Quansah DNK, Baral A, Liang B, Geiger JD Endolysosome Iron Chelation Inhibits HIV-1 Protein-Induced Endolysosome De-Acidification-Induced Increases in Mitochondrial Fragmentation, Mitophagy, and Cell Death. Cells, 11 (2022), pp. 1811. [PubMed: 35681506]

Hara Y, Yuk F, Puri R, Janssen WG, Rapp PR, Morrison JH Presynaptic mitochondrial morphology in monkey prefrontal cortex correlates with working memory and is improved with estrogen treatment. Proc. Natl. Acad. Sci. USA, 111(2014), pp. 486–91. [PubMed: 24297907]

Haughey NJ, Mattson MP Calcium dysregulation and neuronal apoptosis by the HIV-1 proteins Tat and gp120. J. Acquir. Immune Defic. Syndr, 31 Suppl 2 (2002), pp. S55–61. [PubMed: 12394783]

Höke A, Morris M, Haughey NJ GPI-1046 protects dorsal root ganglia from gp120-induced axonal injury by modulating store-operated calcium entry. J. Peripher. Nerv. Syst, 14 (2009), pp. 27–35. [PubMed: 19335537]

Hooper R, Zhang X, Webster M, Go C, Kedra J, Marchbank K, Gill DL, Weeraratna AT, Trebak M, Soboloff J Novel Protein Kinase C-Mediated Control of Orai1 Function in Invasive Melanoma. Mol. Cell. Biol, 35(2015), pp. 2790–8. [PubMed: 26055321]

Hu XT HIV-1 Tat-Mediated Calcium Dysregulation and Neuronal Dysfunction in Vulnerable Brain Regions. Curr. Drug Targets, 17(2016), pp. 4–14. [PubMed: 26028040]

Ivannikov MV, Sugimori M, Llinás RR Synaptic vesicle exocytosis in hippocampal synaptosomes correlates directly with total mitochondrial volume. J. Mol. Neurosci, 49(2013), pp. 223–30. [PubMed: 22772899]

Jadhav S, Nema V HIV-Associated Neurotoxicity: The Interplay of Host and Viral Proteins. Mediators Inflamm. 2021(2021), pp. 1267041. [PubMed: 34483726]

Jia H, Qu M, Fan G, Wu H, Wang L miR-499-5p suppresses C-reactive protein and provides neuroprotection in hypoxic-ischemic encephalopathy in neonatal rat. Neurosci. Res, 161(2020), pp. 44–50. [PubMed: 31812653]

Kanda H, Liu S, Iida T, Yi H, Huang W, Levitt RC, Lubarsky DA, Candiotti KA, Hao S Inhibition of Mitochondrial Fission Protein Reduced Mechanical Allodynia and Suppressed Spinal Mitochondrial Superoxide Induced by Perineural Human Immunodeficiency Virus gp120 in Rats. Anesth. Analg, 122(2016), pp. 264–72. [PubMed: 26418124]

Kashatus DF, Lim KH, Brady DC, Pershing NL, Cox AD, Counter CM RALA and RALBP1 regulate mitochondrial fission at mitosis. Nat. Cell Biol, 13(2011), pp. 1108–1115. [PubMed: 21822277]

Kawamata H, Manfredi G Mitochondrial dysfunction and intracellular calcium dysregulation in ALS. Mech. Ageing Dev, 131(2010), pp. 517–26. [PubMed: 20493207]

Khacho M, Slack RS Mitochondrial dynamics in neurodegeneration: from cell death to energetic states. AIMS Mol. Sci, 2(2015), pp. 161–174.

Kim S, Hahn YK, Podhaizer EM, McLane VD, Zou S, Hauser KF, Knapp PE A central role for glial CCR5 in directing the neuropathological interactions of HIV-1 Tat and opiates. J. Neuroinflammation, 15(2018), pp. 285. [PubMed: 30305110]

Kim SS, Seo SR The regulator of calcineurin 1 (RCAN1/DSCR1) activates the cAMP response element-binding protein (CREB) pathway. J. Biol. Chem, 286(2011), pp. 37841–8. [PubMed: 21890628]

Knott AB, Perkins G, Schwarzenbacher R, Bossy-Wetzel E Mitochondrial fragmentation in neurodegeneration. Nat. Rev. Neurosci, 9(2008), pp. 505–18. [PubMed: 18568013]

Kondadi AK, Anand R, Reichert AS Functional Interplay between Cristae Biogenesis, Mitochondrial Dynamics and Mitochondrial DNA Integrity. Int. J. Mol. Sci, 20(2019), pp. 4311. [PubMed: 31484398]

Krogh KA, Lyddon E, Thayer SA HIV-1 Tat activates a RhoA signaling pathway to reduce NMDA-evoked calcium responses in hippocampal neurons via an actin-dependent mechanism. J. Neurochem, 132(2015), pp. 354–66. [PubMed: 25156524]

Kumar S, Ashraf RCKA. Mitochondrial dynamics regulators: implications for therapeutic intervention in cancer. Cell. Biol. Toxicol, 38 (2022), pp. 377–406. [PubMed: 34661828]

Lai TW, Zhang S, Wang YT Excitotoxicity and stroke: identifying novel targets for neuroprotection. Prog. Neurobiol, 115(2014), pp. 157–88. [PubMed: 24361499]

Liu J, Yang J Mitochondria-associated membranes: A hub for neurodegenerative diseases. Biomed Pharmacother, 149 (2022), pp. 112890. [PubMed: 35367757]

Lu A, Frink M, Choudhry MA, Schwacha MG, Hubbard WJ, Rue LW 3rd, Bland KI, Chaudry IH. Mitochondria play an important role in 17beta-estradiol attenuation of H(2)O(2)-induced rat endothelial cell apoptosis. Am. J. Physiol. Endocrinol. Metab, 292(2007), pp. E585–93. [PubMed: 17018771]

Mallilankaraman K, Cárdenas C, Doonan PJ, Chandramoorthy HC, Irrinki KM, Golenár T, Csordás G, Madireddi P, Yang J, Müller M, Miller R, Kolesar JE, Molgó J, Kaufman B, Hajnóczky G, Foskett JK, Madesh M MCUR1 is an essential component of mitochondrial Ca2+ uptake that regulates cellular metabolism. Nat. Cell. Biol, 14(2012), pp. 1336–43. [PubMed: 23178883]

Nabi SU, Khan A, Siddiqui EM, Rehman MU, Alshahrani S, Arafah A, Mehan S, Alsaffar RM, Alexiou A, Shen B Mechanisms of Mitochondrial Malfunction in Alzheimer's Disease: New Therapeutic Hope. Oxid. Med. Cell. Longev, 2022 (2022), pp. 4759963. [PubMed: 35607703]

Nath A, Padua RA, Geiger JD HIV-1 coat protein gp120-induced increases in levels of intrasynaptosomal calcium. Brain Res, 678(1995), pp. 200–6. [PubMed: 7620888]

Nhu NT, Xiao SY, Liu Y, Kumar VB, Cui ZY, Lee SD Neuroprotective Effects of a Small Mitochondrially-Targeted Tetrapeptide Elamipretide in Neurodegeneration. Front. Integr. Neurosci, 15 (2022), pp. 747901. [PubMed: 35111001]

Otera H, Wang C, Cleland MM, Setoguchi K, Yokota S, Youle RJ, Mihara K Mff is an essential factor for mitochondrial recruitment of Drp1 during mitochondrial fission in mammalian cells. J. Cell. Biol, 191(2010), pp. 1141–58. [PubMed: 21149567]

Potter MC, Figuera-Losada M, Rojas C, Slusher BS Targeting the glutamatergic system for the treatment of HIV-associated neurocognitive disorders. J. Neuroimmune Pharmacol, 8(2013), pp. 594–607. [PubMed: 23553365]

Quiles JM, Gustafsson ÅB The role of mitochondrial fission in cardiovascular health and disease. Nat. Rev. Cardiol, (2022), May 6.

Rom I, Deshmane SL, Mukerjee R, Khalili K, Amini S, Sawaya BE HIV-1 Vpr deregulates calcium secretion in neural cells. Brain Res, 1275(2009), pp. 81–6. [PubMed: 19328187]

Sanchez AB, Medders KE, Maung R, Sánchez-Pavón P, Ojeda-Juárez D, Kaul M CXCL12-induced neurotoxicity critically depends on NMDA receptor-gated and L-type Ca2+ channels upstream of p38 MAPK. J. Neuroinflammation, 13 (2016), pp. 252. [PubMed: 27664068]

Sanderson JL, Gorski JA, Gibson ES, Lam P, Freund RK, Chick WS, Dell'Acqua ML AKAP150-anchored calcineurin regulates synaptic plasticity by limiting synaptic incorporation of Ca^{2+}-permeable AMPA receptors. J. Neurosci, 32(2012), pp. 15036–52. [PubMed: 23100425]

Sanz A, Caro P, Gómez J, Barja G Testing the vicious cycle theory of mitochondrial ROS production: effects of H2O2 and cumene hydroperoxide treatment on heart mitochondria. J. Bioenerg. Biomembr, 38(2006), pp. 121–7. [PubMed: 16841200]

Scheffer DDL, Garcia AA, Lee L, Mochly-Rosen D, Ferreira JCB Mitochondrial Fusion, Fission, and Mitophagy in Cardiac Diseases: Challenges and Therapeutic Opportunities. Antioxid. Redox. Signal, 36 (2022), pp. 844–863. [PubMed: 35044229]

Serasinghe MN, Chipuk JE Mitochondrial Fission in Human Diseases. Handb. Exp. Pharmacol, 240(2017), pp.159–188. [PubMed: 28040850]

Shanmughapriya S, Rajan S, Hoffman NE, Zhang X, Guo S, Kolesar JE, Hines KJ, Ragheb J, Jog NR, Caricchio R, Baba Y, Zhou Y, Kaufman BA, Cheung JY, Kurosaki T, Gill DL, Madesh M Ca2+ signals regulate mitochondrial metabolism by stimulating CREB-mediated expression of the mitochondrial Ca2+ uniporter gene MCU. Sci. Signal, 8(2015), pp. ra23. [PubMed: 25737585]

Sharma A, Ahmad S, Ahmad T, Ali S, Syed MA Mitochondrial dynamics and mitophagy in lung disorders. Life Sci 284 (2021), pp. 119876. [PubMed: 34389405]

Shrestha J, Santerre M, Allen CNS, Arjona SP, Merali C, Mukerjee R, Chitrala KN, Park J, Bagashev A, Bui V, Eugenin EA, Merali S, Kaul M, Chin J, Sawaya BE HIV-1 gp120 Impairs Spatial Memory Through Cyclic AMP Response Element-Binding Protein. Front. Aging Neurosci, 14 (2022), pp. 811481. [PubMed: 35615594]

Smalheiser NR, Lugli G, Zhang H, Rizavi H, Cook EH, Dwivedi Y Expression of microRNAs and other small RNAs in prefrontal cortex in schizophrenia, bipolar disorder and depressed subjects. PLoS One, 9(2014), pp. e86469. [PubMed: 24475125]

Spurlock B, Tullet J, Hartman JL 4th, Mitra K Interplay of mitochondrial fission-fusion with cell cycle regulation: Possible impacts on stem cell and organismal aging. Exp. Gerontol, 135 (2020), pp. 110919. [PubMed: 32220593]

Tangmansakulchai K, Abubakar Z, Kitiyanant N, Suwanjang W, Leepiyasakulchai C, Govitrapong P, Chetsawang B Calpastatin overexpression reduces oxidative stress-induced mitochondrial impairment and cell death in human neuroblastoma SH-SY5Y cells by decreasing calpain and calcineurin activation, induction of mitochondrial fission and destruction of mitochondrial fusion. Mitochondrion, 30(2016), pp. 151–61. [PubMed: 27453331]

Teodorof-Diedrich C, Spector SA Human Immunodeficiency Virus Type 1 gp120 and Tat Induce Mitochondrial Fragmentation and Incomplete Mitophagy in Human Neurons. J. Virol, 92(2018), pp. e00993–18. [PubMed: 30158296]

Toggas SM, Masliah E, Rockenstein EM, Rall GF, Abraham CR, Mucke L Central nervous system damage produced by expression of the HIV-1 coat protein gp120 in transgenic mice. Nature, 367 (1994), pp. 188–93. [PubMed: 8114918]

Tomar D, Dong Z, Shanmughapriya S, Koch DA, Thomas T, Hoffman NE, Timbalia SA, Goldman SJ, Breves SL, Corbally DP, Nemani N, Fairweather JP, Cutri AR, Zhang X, Song J, Jaña F, Huang J, Barrero C, Rabinowitz JE, Luongo TS, Schumacher SM, Rockman ME, Dietrich A, Merali S, Caplan J, Stathopulos P, Ahima RS, Cheung JY, Houser SR, Koch WJ, Patel V, Gohil VM, Elrod JW, Rajan S, Madesh M MCUR1 Is a Scaffold Factor for the MCU Complex Function and Promotes Mitochondrial Bioenergetics. Cell Rep, 15(2016), pp. 1673–85. [PubMed: 27184846]

Uchikado Y, Ikeda Y, Ohishi M Current Understanding of the Pivotal Role of Mitochondrial Dynamics in Cardiovascular Diseases and Senescence. Front. Cardiovasc. Med, 9 (2022), pp. 905072. [PubMed: 35665261]

Wang JX, Jiao JQ, Li Q, Long B, Wang K, Liu JP, Li YR, Li PF miR-499 regulates mitochondrial dynamics by targeting calcineurin and dynamin-related protein-1. Nat. Med, 17(2011), pp. 71–8. [PubMed: 21186368]

Wang X, Wu C Tanshinone IIA improves cardiac function via regulating miR-499-5p dependent angiogenesis in myocardial ischemic mice. Microvasc. Res, 143(2022), pp. 104399. [PubMed: 35697130]

Wang Z, Jiang H, Chen S, Du F, Wang X The mitochondrial phosphatase PGAM5 functions at the convergence point of multiple necrotic death pathways. Cell, 148(2012), pp. 228–243. [PubMed: 22265414]

Wang Z, Pekarskaya O, Bencheikh M, Chao W, Gelbard HA, Ghorpade A, Rothstein JD, Volsky DJ Reduced expression of glutamate transporter EAAT2 and impaired glutamate transport in human primary astrocytes exposed to HIV-1 or gp120. Virology, 312(2003), pp. 60–73. [PubMed: 12890621]

Weissman D, Rabin RL, Arthos J, Rubbert A, Dybul M, Swofford R, Venkatesan S, Farber JM, Fauci AS Macrophage-tropic HIV and SIV envelope proteins induce a signal through the CCR5 chemokine receptor. Nature, 389(1997), pp. 981–5. [PubMed: 9353123]

Wiemerslage L, Lee D Quantification of mitochondrial morphology in neurites of dopaminergic neurons using multiple parameters. J. Neurosci. Methods, 262(2016), pp. 56–65. [PubMed: 26777473]

Xu H, Bae M, Tovar-y-Romo LB, Patel N, Bandaru VV, Pomerantz D, Steiner JP, Haughey NJ The human immunodeficiency virus coat protein gp120 promotes forward trafficking and surface clustering of NMDA receptors in membrane microdomains. J. Neurosci. 31(2011), pp. 17074–90. [PubMed: 22114277]

Xue C, Dong N, Shan A Putative role of STING-mitochondria associated membrane crosstalk in immunity. Trends Immunol, S1471–4906 (2022), pp. 00097–7.

Ye X, Zhang Y, Xu Q, Zheng H, Wu X, Qiu J, Zhang Z, Wang W, Shao Y, Xing HQ HIV-1 Tat inhibits EAAT-2 through AEG-1 upregulation in models of HIV-associated neurocognitive disorder. Oncotarget, 8(2017), pp. 39922–39934. [PubMed: 28404980]

Youle RJ, van der Bliek AM Mitochondrial fission, fusion, and stress. Science, 337 (2012), pp. 1062–5. [PubMed: 22936770]

Zeng Y, Wang L, Zhou Y, Liang M, Yu J, Wu S, Zhou Y NMDA receptor antagonists engender neuroprotection against gp120-induced cognitive dysfunction in rats through modulation of PKR activation, oxidative stress, ER stress and IRE1α signal pathway. Eur. J. Neurosci, 2022 May 11.

Zhang W, Li J, Yao H, Li T Restoring microRNA-499–5p Protects Sepsis-Induced Lung Injury Mice Via Targeting Sox6. Nanoscale Res. Lett, 16(2021), pp. 89. [PubMed: 34019224]

Zhou Y, Liu J, Xiong H HIV-1 Glycoprotein 120 Enhancement of N-Methyl-D-Aspartate NMDA Receptor-Mediated Excitatory Postsynaptic Currents: Implications for HIV-1-Associated Neural Injury. J. Neuroimmune Pharmacol, 12(2017), pp. 314–326. [PubMed: 28005232]

Highlights

- A novel and unknown mechanism that implicates miR-499-5p used by HIV-1 gp120 protein leading to neuronal deregulation premature aging.
- gp120 protein disrupts mitochondrial functions, shape, and size through the activation of the calcineurin pathway.
- Gp120 effect was neutralized in the presence of miR-499-5p, an upstream effector of calcineurin.
- We propose a novel therapy based on miR-499 activation.

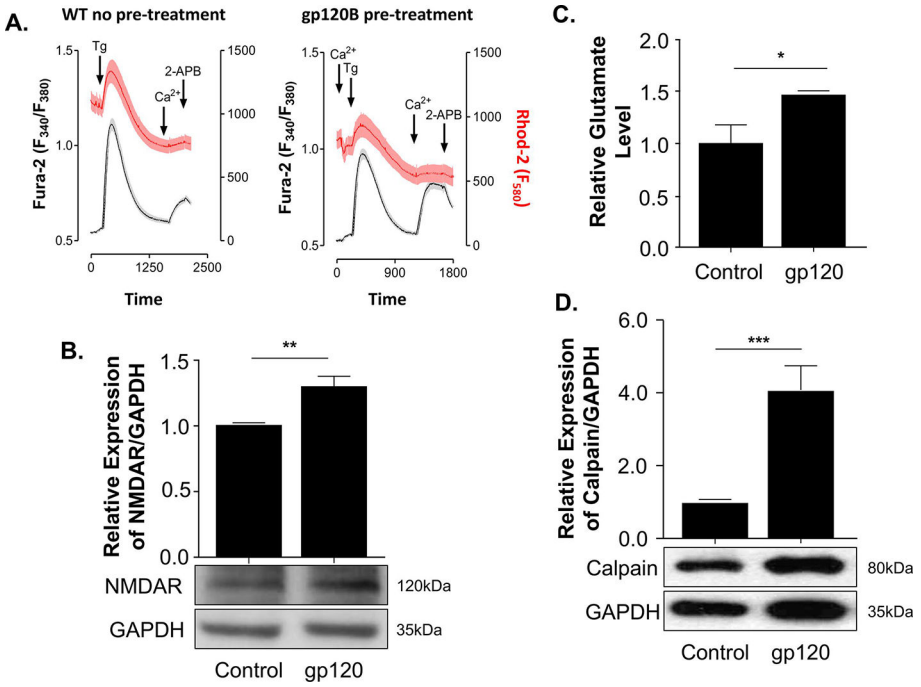

Figure 1. HIV-1 gp120 treatment leads to increased NMDAR expression and glutamate levels.

(A) Cytosolic and mitochondrial Ca^{2+} levels were measured using a ratiometric dye Fura2-AM (Grey) and Rhodamine (Red) for the cytosolic and mitochondrial Ca^{2+}. Expression levels of NMDAR **(B)** and Calpain **(D)** isolated from untreated or gp120-treated SH-SY5Y as obtained by western blot assays, respectively. Quantitative analysis of the western blot was presented along with the bands as a bar graph. The data shown are from a single experiment (n-3) and were statistically significant. GAPDH represents the loading control. **(C)** Relative glutamate level was measured using a plate reader at O.D. 450 nm for different treatment conditions. The experiments were done in triplicate and the *p* values were calculated using the Student *t*-test (mean ± S.D.) (*p<0.05; **p<0.01; ***p<0.001).

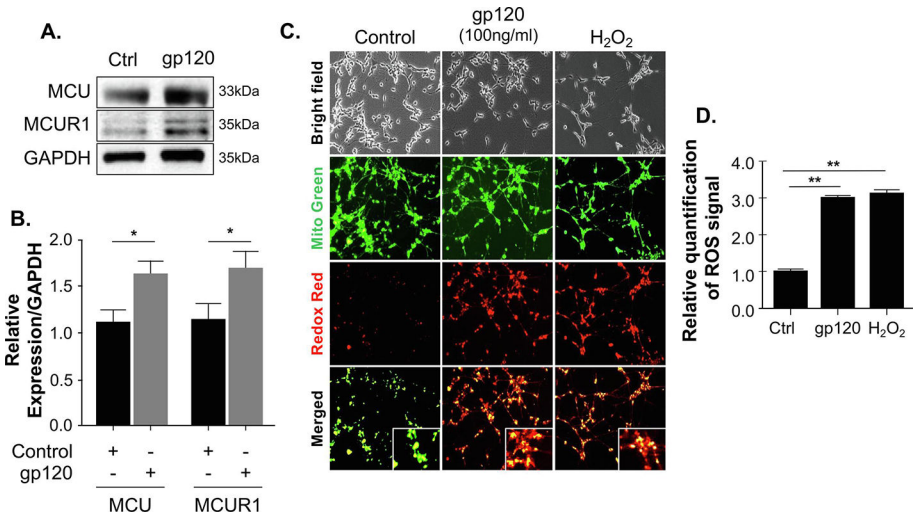

Figure 2. An aberrant expression of MCU proteins in gp120-treated cells

(A) Expression levels of MCU complex proteins (MCU and MCUR1) isolated from untreated or gp120-treated SH-SY5Y as obtained by western blot assays. GAPDH represents the loading control. **(B)** Bar graphs represent the quantitative analysis of the western blot. The data shown are from a single experiment (n=3) and were statistically significant. Data represent the mean ± S.D. Results were judged statistically significant if $p < 0.05$ by analysis of variance. **(C)** Representative images of RedoxSensor (red) and MitoTracker (green) staining for ROS in differentiated SH-SY5Y cells treated with 100ng/ml of gp120 for 24 hours or H_2O_2. ROS production is seen by the colocalization of the two dyes in the mitochondria. Data shown here are from a single that was replicated 3 times and were statistically significant. **(D)** Quantification of ROS signal in panel D using the Student t-test. Data were statistically significant ($p<0.05$) when comparing gp120-treated cells to the control (Ctrl) group (one-way ANOVA).

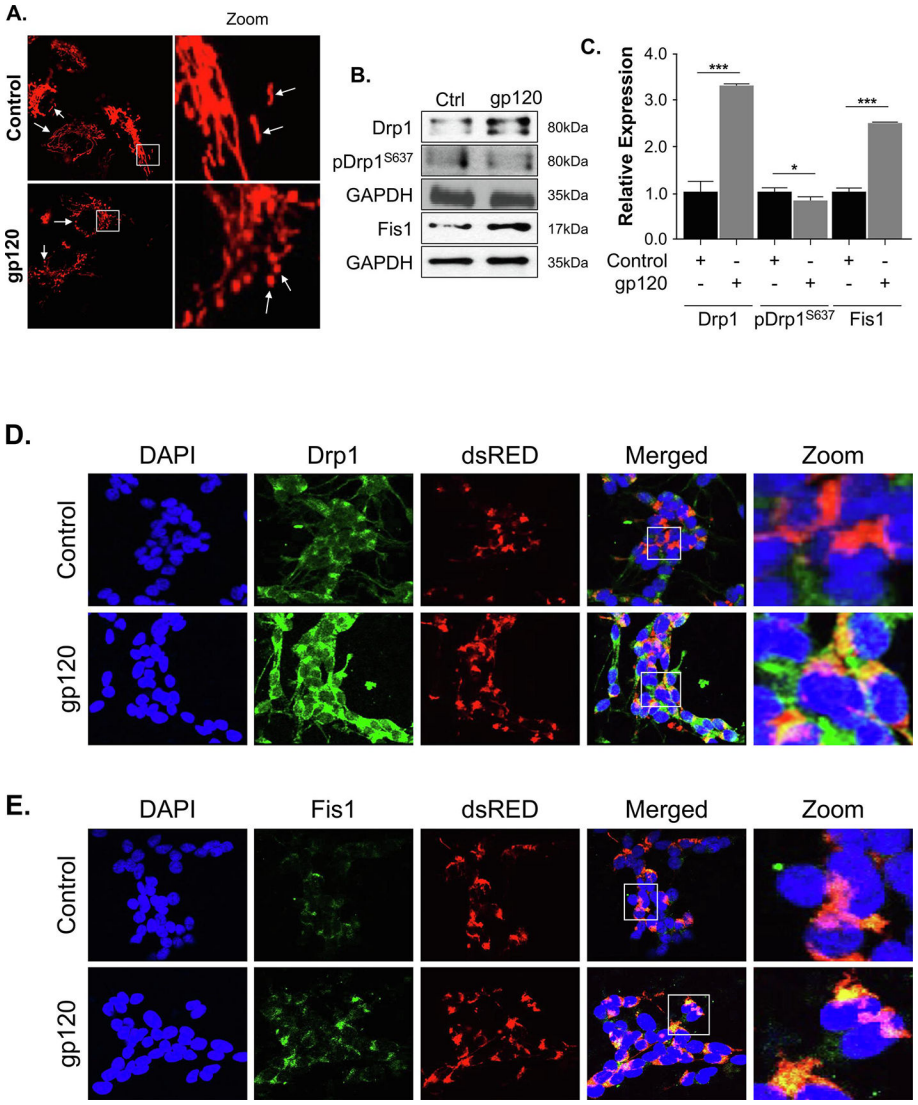

Figure 3. HIV-1 gp120 alters the mitochondrial shape and Drp1 and Fis1 expression levels.

(A) SH-SY5Y cells were transfected with a pDsRed2-Mito expression plasmid for 24 hours and then differentiated for 3 days. The cells were then treated with 100ng/ml of recombinant gp120 protein for an additional 24 hours. Images of the mitochondria were captured using Leica EL600 DMI3000 confocal microscopy 63x lenses. The rod-shaped elongated mitochondria are the healthy mitochondria and the rounded mitochondria seen in gp120-treated cells indicate the swelling of mitochondria and possible increased fission. **(B)** The western blot analysis represents the protein expressions of total Drp1, phosphor-Drp1^{S637}, and Fis1. GAPDH was used as a loading control. **(C)** Quantitative analysis of the western blot was presented along with the bands. Data represent the mean ± S.D. Results were judged statistically significant if $p<0.05$ by analysis of variance. (*p<0.05; **p<0.01; ***p<0.001). **(D, E)** SH-SY5Y cells were plated on the glass chamber slides followed by transfection with pDsRed2-Mito to label the mitochondria, differentiated for 3 days, then treated with gp120 for an additional 24 hours. An immunocytochemistry assay was performed using anti-Drp1 (**D**) or anti-Fis1 (**E**) antibodies. Mitochondria are labeled in red,

Drp1 or Fis1 are green, and DAPI (blue) was used to label the nuclei. Colocalization of the proteins with mitochondria is indicated by the presence of an orange or yellow signal (zoom). (Control = Ctrl)

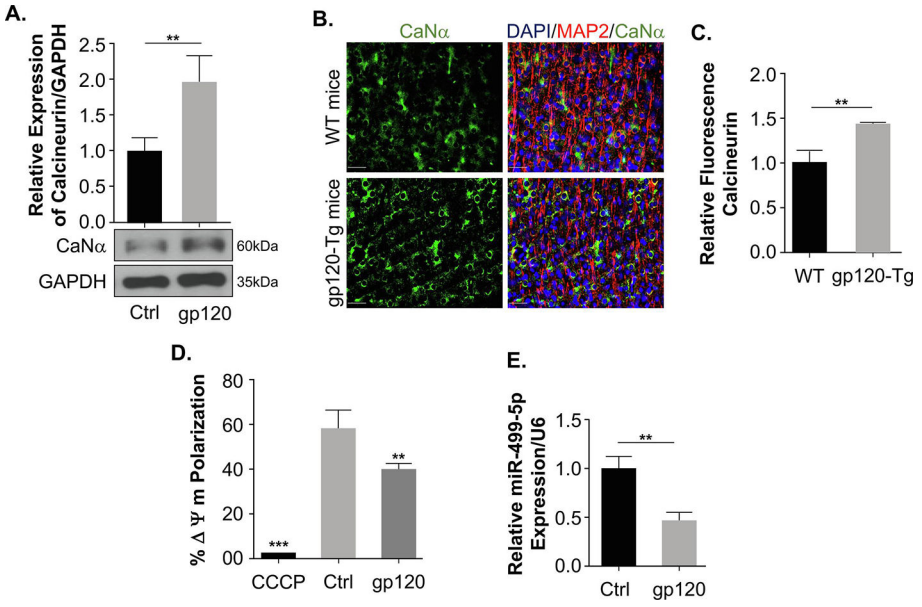

Figure 4. Calcineurin and miR-499-5p expression in the presence of HIV-1 gp120.

(A) The whole cell extract was subjected to the western blot analysis showing the protein expression of Calcineurin in untreated control and gp120 treated for 24 hours. Quantitative analysis of the western blot was presented along with the bands. **(B)** The immunohistochemistry and the quantitation of the fluorescence of the frontal cerebral cortex layer III (no neighbor deconvolution, scale bar = 40 μm) brain slides of a 9-month-old gp120-Tg mouse (HPX1481) and the age-matched control (HPX1477). Calcineurin – green; MAP-2 – red; and nuclei – blue (DAPI). **(C)** Quantitative analysis of fluorescent calcineurin was presented as a bar graph. **(D)** Mitochondrial membrane potential change was measured using JC-1 dye on differentiated SH-SY5Y cells subjected to different treatment conditions using a Guava Flow cytometer. CCCP was used as a control to determine the mitochondrial membrane potential collapse. (**E**) The relative expression of miR-499-5p normalized to an internal control U6. Data represent the mean ± S.D. Results were judged statistically significant if $p<0.05$ by analysis of variance. (*p<0.05; **p<0.01; ***p<0.001). (Control=Ctrl).

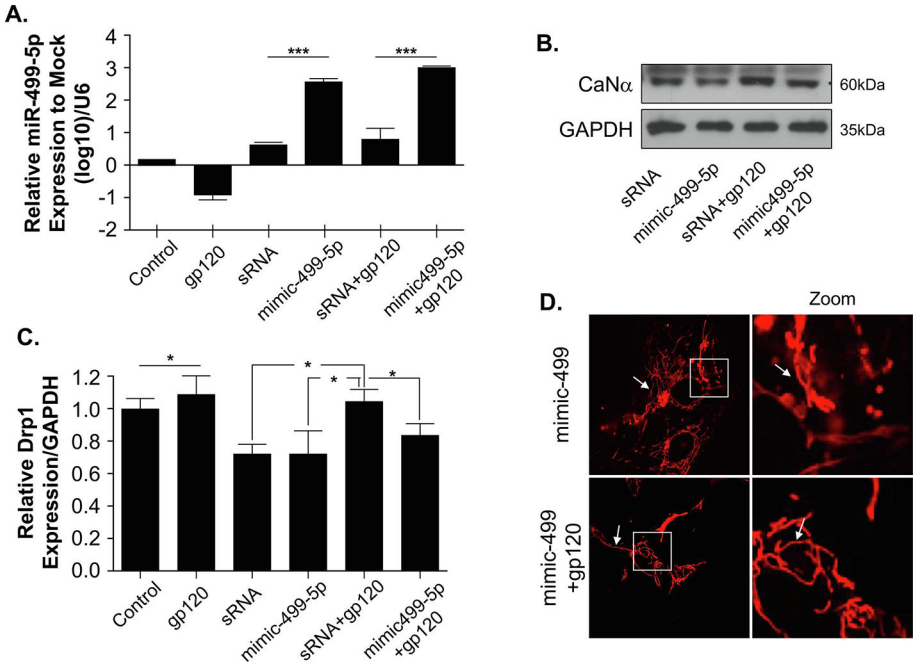

Figure 5. Overexpression of miR-499-5p neutralizes the gp120 effect.

(A) Relative expression of miR-499-5p normalized to the untreated control (log10) indicating the overexpression of miR-499-5p using a mimic-499-5p and U6 as an internal loading control. **(B)** Overexpression of miR-499-5p led to inhibition in Calcineurin expression, thus rescuing the effect of gp120. **(C)** Relative DRP1 expression level normalized to internal control. The GAPDH represents the effect of overexpressed miR-499-5p that caused the inhibition of calcineurin and decreased expression of Drp1. Data represent the mean ± S.D. Results are statistically significant ($p<0.05$ by analysis of variance, *p<0.05; **p<0.01; ***p<0.001). **(D)** Cells transfected with miR-499-5p displayed elongated mitochondrial structure and rescued the effect of gp120. (Control=Ctrl)

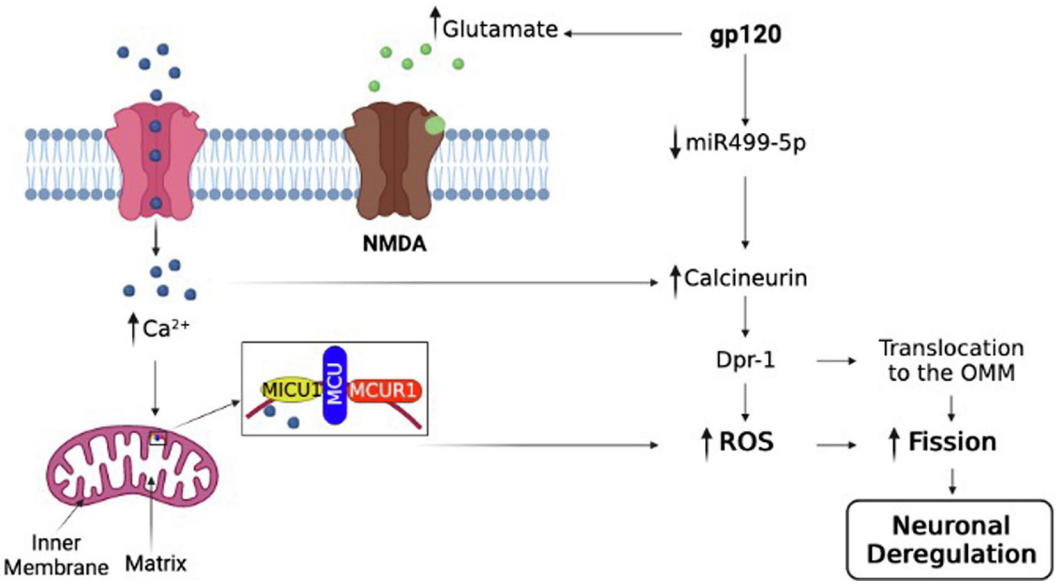

Figure 6. The potential pathway used by gp120.

A schematic representation of the possible pathway involved in gp120-mediated mitochondrial shape deregulation that leads to neurocognitive disorders such as spatial memory impairment (cartoon created using BioRender.com software).